

Temperature signature of high latitude Atlantic boundary currents revealed by marine mammal-borne sensor and Argo data

Jeremy P. Grist,¹ Simon A. Josey,¹ Lars Boehme,² Michael P. Meredith,³
Fraser J. M. Davidson,⁴ Garry B. Stenson,⁴ and Mike O. Hammill⁵

Received 20 May 2011; revised 17 June 2011; accepted 21 June 2011; published 2 August 2011.

[1] Results from the development and analysis of a novel temperature dataset for the high latitude North-West Atlantic are presented. The new 1° gridded dataset (“ATLAS”) has been produced from about 13,000 Argo and 48,000 marine mammal (hooded seal, harp seal, grey seal and beluga) profiles spanning 2004–8. These data sources are highly complementary as marine mammals greatly enhance shelf region coverage where Argo floats are absent. ATLAS reveals distinctive boundary current related temperature minima in the Labrador Sea (−1.1°C) and at the east Greenland coast (1.8°C), largely absent in the widely-used Levitus’09 and EN3v2a datasets. The ATLAS 0–500 m average temperature is lower than Levitus’09 and EN3v2a by up to 3°C locally. Differences are strongest from 0–300 m and persist at reduced amplitude from 300–500 m. Our results clearly reveal the value of marine mammal-borne sensors for a reliable description of the North-West Atlantic at a time of rapid change. **Citation:** Grist, J. P., S. A. Josey, L. Boehme, M. P. Meredith, F. J. M. Davidson, G. B. Stenson, and M. O. Hammill (2011), Temperature signature of high latitude Atlantic boundary currents revealed by marine mammal-borne sensor and Argo data, *Geophys. Res. Lett.*, 38, L15601, doi:10.1029/2011GL048204.

1. Introduction

[2] The high latitude North-West Atlantic is an important region of water mass formation, which exerts influence not only on the large-scale ocean circulation, but ultimately on planetary-scale climate. Upper North Atlantic Deep Water (NADW), formed via intense air-sea heat exchange in the central Labrador Sea, combines with Lower NADW from the Arctic Seas to form the deep southward-flowing water masses of the Atlantic Meridional Overturning Circulation. The region is also a conduit for the relatively swift passage of very cool and fresh surface water of Nordic and Arctic origin to the sub-polar ocean via the East Greenland Current (EGC), the West Greenland Current and the Labrador Current.

[3] Understanding variability in the region’s export of NADW and the strength and character of the coastal currents is made challenging by the complex array of processes at work. These include the existence of the on-shelf East

Greenland Coastal Current (EGCC) [Bacon *et al.*, 2002], the partial retroflexion of the EGC at Cape Farewell [Holliday *et al.*, 2007] and the generation and cross-basin transport of eddies [Chanut *et al.*, 2008]. Furthermore, the dramatic reduction in Arctic sea-ice cover observed in recent years [Stroeve *et al.*, 2007] is likely to impact the region, making accurate determination of its properties and their ongoing changes a high priority.

[4] A key step towards understanding North-West Atlantic variability is a reliable determination of the mean temperature characteristics to serve as a baseline against which changes can be robustly determined. This is particularly important in the context of high-resolution ocean-only model studies: these are typically initiated from a temperature-salinity basic state and relaxed back to this state during the course of an integration to eliminate excessive drift. However, the global climatologies used most frequently for this purpose [e.g., Levitus *et al.*, 1998] have a limited depiction of important coastal currents [Kulan and Myers, 2009], and consequently may inadvertently promote, rather than restrict, model drift [Rattan *et al.*, 2010]. This shortcoming is possibly due to the absence of Argo profiling floats (a key source of sub-surface data in these climatologies) from the shelf regions, as well as the fact that data acquired by research vessels in these regions are strongly seasonal in nature due to the challenges of working in ice-infested waters.

[5] A novel method to increase observation density in the North-West Atlantic shelf regions is the deployment of marine mammal-borne sensors. To date, such sensors have been utilized in several studies including: characterising the Antarctic Circumpolar Current [Boehme *et al.*, 2008a], estimating sea-ice formation rates [Charrassin *et al.*, 2008], defining seasonal temperature variations on the East Greenland Shelf [Straneo *et al.*, 2010] and studying temperature variability in Baffin Bay [Laidre *et al.*, 2010]. However, their potential to produce gridded datasets in key regions has yet to be fully exploited. Here, we fill this gap by producing and analysing a new 1° gridded North-West Atlantic temperature dataset using marine mammal and Argo float measurements; the dataset reveals important features not seen in earlier analyses with poorer sampling.

2. Data and Method

[6] The new dataset spans the region 40°N–75°N, 70°W–20°W (black box, Figure 1a) and employs Argo and marine mammal data from 2002–2009. The Argo data have all passed Argo delayed mode quality control (QC); additionally only data with temperature, pressure, location and time quality control flags of 1 (‘Good Data’) were included. Argo floats profile down to 2000 m once every 8–10 days. After

¹National Oceanography Centre, Southampton, UK.

²Sea Mammal Research Unit, University of St. Andrews, Saint Andrews, UK.

³British Antarctic Survey, Cambridge, UK.

⁴Fisheries and Oceans Canada, St. John’s, Newfoundland, Canada.

⁵Maurice Lamontagne Institute, Fisheries and Oceans Canada, Mont-Joli, Quebec, Canada.

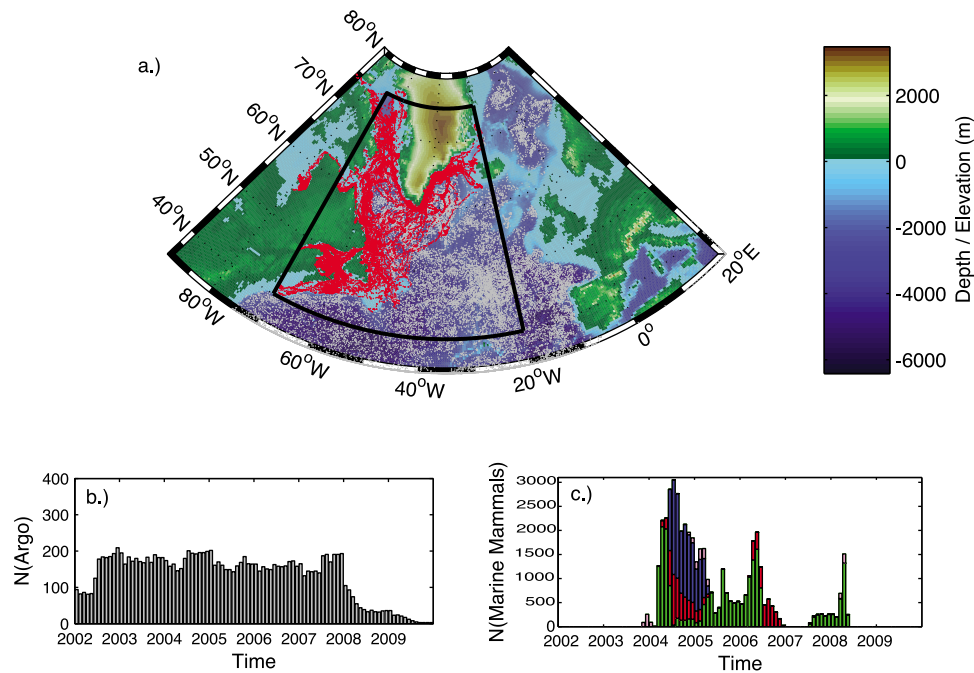


Figure 1. (a) Distribution of temperature profiles from Argo (grey dots) and marine mammal-mounted sensors (red dots). Monthly number, N , of (b) Argo and (c) marine mammal (hooded seals, green; harp seals, red; grey seals, blue; beluga, pink) profiles in the study area (black box in Figure 1a).

QC there were 12,623 Argo profiles in our study region. The temperature profiles collected from marine mammal-mounted autonomous Satellite Relay Data Loggers (SRDLs) [Boehme *et al.*, 2009] result from tagging of hooded seals, harp seals, grey seals and beluga whales by Fisheries and Oceans Canada off east Greenland, the Newfoundland Shelf, the Gulf of St. Lawrence and Hudson Bay respectively between July 2003 and May 2008 [e.g., Andersen *et al.*, 2010] (Figure 1c). Full details of the data retrieval process and quality control are given in the auxiliary material.¹

[7] The Argo and marine mammal data distributions are shown in Figure 1. Some overlap is seen, particularly in the central Labrador and Irminger Basins, however their complementary spatial coverage is striking. The addition of marine mammal data to Argo approximately quintuples the number of profiles for the region. We have focused on Argo and marine mammal data as this enables us to develop a dataset complementary to existing ship-based fields, and thereby identify their potential issues and limitations. For example, ship-based hydrographic data contain strong seasonal biases in shelf regions due to the timing of their collection (see Figure S3 in the auxiliary material) and our goal is to use data without this bias in order to generate a dataset more representative of a genuine annual mean. Previous work conducted using this technique (most notably in the South Atlantic [e.g., Boehme *et al.*, 2008a]) has also employed merged Argo and marine mammal sensor data without incorporating ship-derived hydrography, for this same reason of seasonal bias in the latter data source.

[8] For each month from January 2004 to December 2008, a gridded temperature field and objective analysis (OA) error

is produced for the study region using the OA scheme and representative regional correlation scales from Boehme and Send [2005]. In producing a grid cell estimate, the scheme weights all observations according to separation from the grid point in terms of a) horizontal distance, b) barotropic potential vorticity (to allow for topographic steering of currents) and c) time from the middle of the month. As the method allows monthly grid cell estimates to be influenced by observations from beyond both the spatial bounds of the grid box and the temporal bounds of the specific month, the source data has a larger time and space domain (Figure 1) than the resulting analysed gridded fields. The OA error reflects the degree of separation (in time, distance and potential vorticity) of a grid point from the observations, such that the error estimate becomes smaller as the number of nearby observations increases [Boehme and Send, 2005].

[9] The monthly values are then averaged to produce the mean state for 2004–2008. The grid resolution is $1^\circ \times 1^\circ$ with 15 vertical layers from 0–700 m. These grid parameters have been chosen to allow direct comparison with the mean fields for 2004–08 from Levitus *et al.*'s [2009, hereafter L09] dataset. L09's product consists of annual anomaly fields and an associated long-term climatological mean field; to produce the 2004–08 mean used for the present work we added the 5 annual anomaly fields for this time interval to the climatological mean field. The only difference from L09's product is that, in our analysis, the top two ocean levels (0–5 m and 5–15 m) are merged due to the reduced availability of profiling observations at these depths. We also compare our estimate with the 2004–08 mean temperature derived from the EN3 (version 2a) potential temperature and salinity product from the UK Met Office Hadley Centre [Ingleby and Huddleston, 2007]. The EN3 product consists of gridded mean fields for each individual month, we produced the estimate of the 2004–08 EN3 mean used for this study, shown in Figure 2, by

¹Auxiliary materials are available in the HTML. doi:10.1029/2011GL048204.

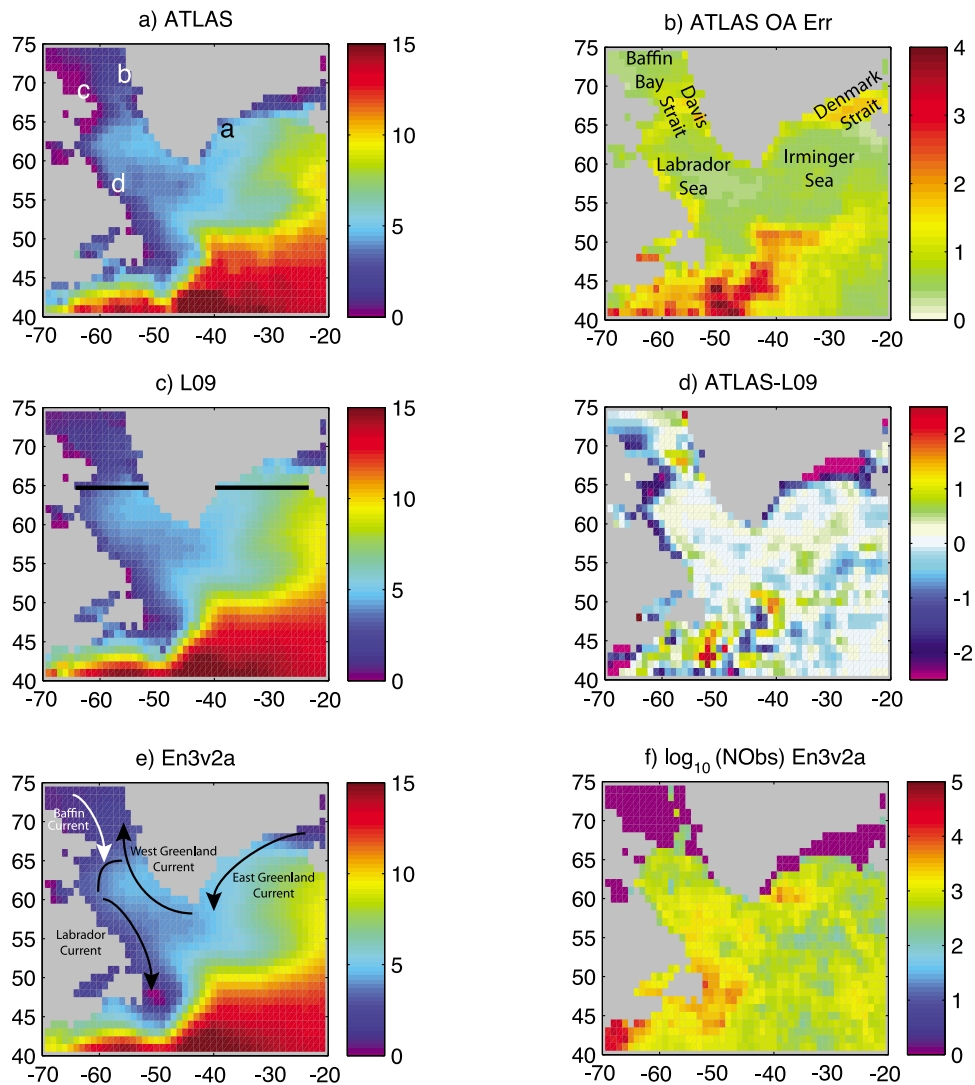


Figure 2. Maps showing the 2004–08 annual mean temperature ($^{\circ}\text{C}$) averaged over 0–500 m for (a) ATLAS, (c) L09 and (e) EN3. (b) OA error ($^{\circ}\text{C}$) for the ATLAS temperature field shown in Figure 2a. (d) The difference, ATLAS - L09, of the temperature fields shown in Figures 2a and 2c. (f) The number of observations (top 500 m) used in EN3 on a \log_{10} scale. The letters in Figure 2a refer to profiles examined in Figure 4 and the section shown in Figure 2c is that used in Figure 3. The key boundary currents are shown schematically in Figure 2e.

averaging the EN3 individual monthly values during this period. EN3 also has 1° horizontal resolution, but with a different configuration. Our new combined Argo and marine mammal sensor dataset is hereafter termed ATLAS (*A Novel Temperature Dataset for Northern High Latitude Seas*).

3. Results

3.1. Mean Fields: Comparison With L09 and EN3

[10] The 2004–2008 mean temperature, averaged over 0–500 m, from ATLAS, and associated OA error, are shown in Figures 2a and 2b. The 2004–08 mean temperature fields from L09 and EN3 are shown in Figures 2c and 2e), while the difference (ATLAS minus L09) is shown in Figure 2d (the ATLAS minus EN3 difference field is similar and not shown). There are important differences between the three datasets in the coastal regions. ATLAS is 1.7°C (2.3°C) cooler than L09 (EN3) in the western parts of Baffin Bay, 2.2°C (2.9°C) cooler in the western Labrador Sea and 1.2°C

(0.9°C) cooler along the Irminger Sea coast. Furthermore, there is a broad region from $65\text{--}70^{\circ}\text{N}$ east of Greenland, in Denmark Strait, where ATLAS has temperatures up to 3°C lower than L09 and EN3. The differences between ATLAS and both L09 and EN3 occur in regions densely sampled by marine mammals and typically exceed the OA error, indicating that they are genuine features not previously recognised by L09 or EN3. The total number of observations from EN3 is shown in Figure 2f; the Denmark Strait and Baffin Bay regions have very low sampling. In such regions EN3 (and L09) will tend toward their respective long-term (multi-decadal) means as opposed to the 2004–08 state we seek to estimate here.

[11] We have also considered the depth-averaged temperature for each 100 m interval within the 0–500 m range (see auxiliary material), within which the differences are strongest in the top 300 m and persist at reduced amplitude from 300–500 m (see discussion below). As well as contrasting data sources, these differences will be partially associated with

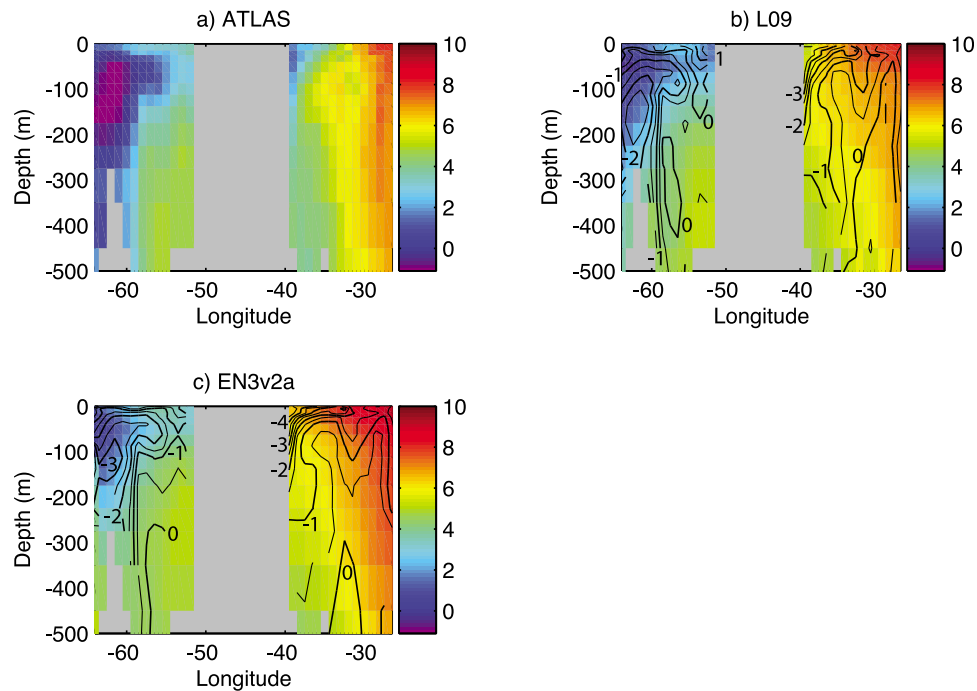


Figure 3. Coloured field: Longitude–depth section of 2004–08 annual mean temperature ($^{\circ}\text{C}$) at 64.5°N for (a) ATLAS, (b) L09 and (c) EN3. Contours show the difference of these fields for Figure 3b, ATLAS - L09, and Figure 3c, ATLAS - EN3, contour intervals 0.5°C , integer contour values are labelled. To aid comparison, EN3 was re-gridded on to the ATLAS grid.

differences in the quality control and objective analysis methods used in constructing L09 and EN3. In contrast to the strong differences on the shelf, ATLAS is in good agreement with L09 and EN3 over most of the deep ocean.

3.2. Comparison of Vertical Structure

[12] For each dataset, the 0–500 m temperature field along a section at 64.5°N (denoted on Figure 2c) adjacent to the Davis and Denmark Straits is shown in Figure 3 (coloured field, with ATLAS minus L09 and ATLAS minus EN3 represented by contours). These fields reveal the vertical structure of the differences between ATLAS and L09 (EN3) at two main locations. First, near the east Greenland coast ($\sim 40^{\circ}\text{W}$), ATLAS exhibits a temperature minimum of 1.8°C at the surface that is absent from L09 and EN3, which have values there of 5.0°C and 6.4°C respectively. In contrast to L09 and EN3, the ATLAS minimum is within the range of hydrographic observations from the region and resembles the temperature signature of the EGC and the EGCC [Rudels *et al.*, 2002; Sutherland and Pickart, 2008]. We note that because the temperature (and salinity) ranges of the EGC and the EGCC can overlap, and because of their close proximity, estimates of velocity (not provided by ATLAS) may be necessary to distinguish them [Sutherland and Pickart, 2008]. Second, although all three datasets have a temperature minimum in the far west of the Labrador Basin (62°W) between 50 and 150 m, this minimum is much colder in ATLAS (minimum value $-1.1 \pm 0.5^{\circ}\text{C}$) than in L09 (minimum -0.3°C) and EN3 (minimum 0.4°C). The ATLAS temperature values for this feature, associated with the southward exit of cold water through Davis Strait in the Baffin Island Current, are closer to the ship-based hydrographic profiles (-1.5°C) of Cuny *et al.* [2005]. Thus, by utilizing marine mammal-sensor data, ATLAS is able to

capture the temperature signature of boundary currents previously recognised in hydrographic surveys that are largely absent in other climatological datasets of comparable resolution. The improved ability to depict these boundary currents is consistent with the behaviour of other marine mammal species, such as southern elephant seals, which have been shown to preferentially sample frontal regions [Boehme *et al.*, 2008b]; hooded seals and harp seals show similar behaviour.

[13] We explore the vertical variation further in Figure 4 by comparing temperature profiles from each dataset at four coastal locations (south-east Greenland, east Baffin Bay, west Baffin Bay and south-west Labrador Sea) shown in Figure 2a. At each location, ATLAS has a cooler surface or sub-surface temperature minimum consistent with a more comprehensive depiction of the cold boundary currents. The data sets differ most at the surface for the south-east Greenland location, where ATLAS has a temperature of 2.6°C , compared to 6.4°C and 5.8°C for L09 and EN3 respectively. Furthermore, in ATLAS, this south-east Greenland surface temperature represents a local minimum in the vertical profile, while in L09 and EN3 the surface temperature are local maxima in their respective vertical profiles. At the other locations, temperature minima occur at approximately 50–100 m and have been interpreted as the remnant of winter cooling, typically on the coastward flank of the boundary current [e.g., Tang *et al.*, 2004; Fratantoni and Pickart, 2007]. In ATLAS the more marked temperature minima, for example 0.1°C compared with 1.8°C (both L09 and EN3) at the south-west Labrador Sea site, are more in accord with nearby hydrographic observations that indicate a substantial amount of water cooler than 0°C [Fratantoni and Pickart, 2007]. The distinctive features of the ATLAS temperature profiles should be considered in the context of the OA error estimates (dashed black lines in Figure 4). L09 and EN3 temperature

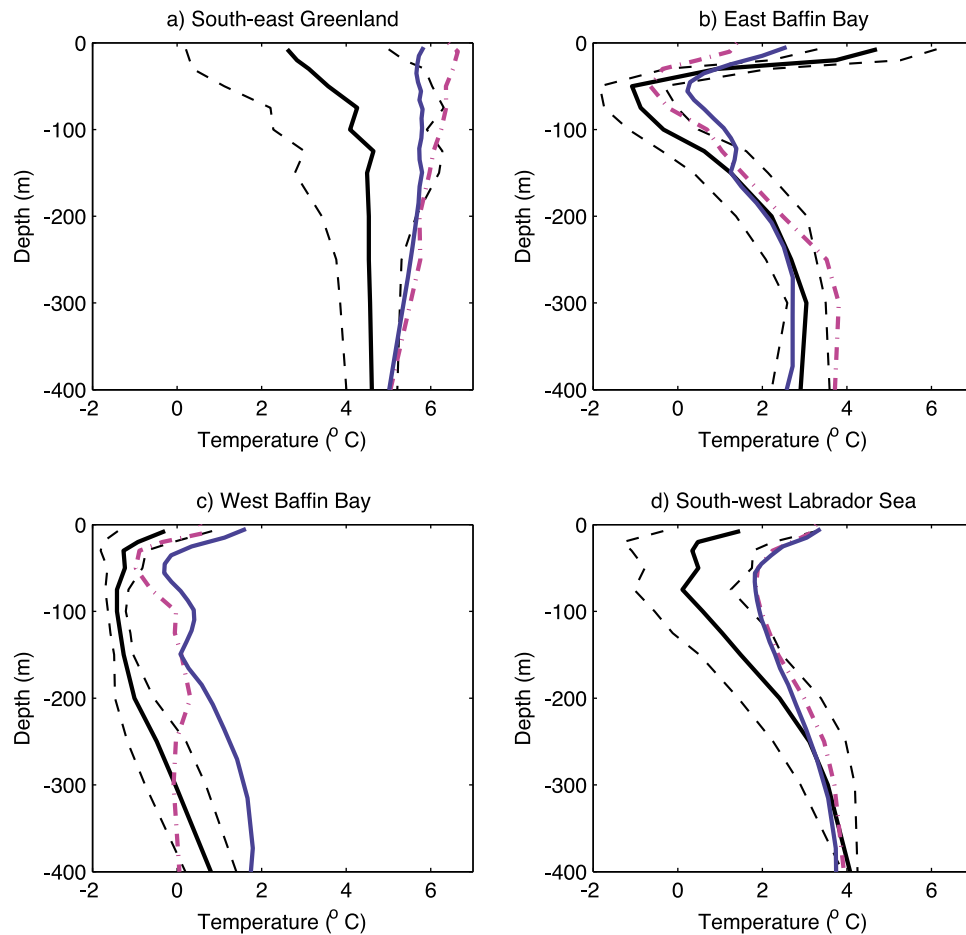


Figure 4. The 2004–8 annual mean temperature profiles at the 4 locations (1° grid cells) of the North-West Atlantic shown in Figure 2a); (a) South-east Greenland (39.5°W , 63.5°N), (b) East Baffin Bay (57.5°W , 70.5°N), (c) West Baffin Bay (64.5°W , 68.5°N), (d) South-west Labrador Sea (58.5°W , 56.5°N): ATLAS (black solid line) with associated OA error (black dashed line); EN3 (solid blue line) and L09 (dashed magenta line).

estimates tend to fall outside the ATLAS OA error range in the top 100 m, at and above the depth of minimum temperature, confirming the physical significance of these differences. Below 300 m, the different profiles (with the exception of west Baffin Bay) tend to converge to within the OA error range. We also note that in some areas (south-east Greenland and south-west Labrador Sea) the near surface OA error estimates remain quite large, indicating that a future increase in observations from marine mammals or other observations would benefit the accuracy of the temperature fields.

4. Conclusions

[14] In the high latitude North-West Atlantic, existing temperature (and salinity) climatologies suffer from a weak representation of boundary current systems [Kulan and Myers, 2009]. This limitation reflects sparse data coverage, particularly in shelf regions that are not sampled by Argo profiling floats. A potential solution to the sampling problem is the use of sensors deployed on marine mammals. Between 2004 and 2008, marine mammal mounted sensors increased the number of profiles in the region five-fold, providing much improved coverage in the formerly data-sparse shelf regions. We have combined this data with Argo float profiles to pro-

duce a new 1° gridded temperature dataset for the region 40°N – 75°N , 70°W – 20°W .

[15] Our analysis of the new dataset reveals cold temperature signals in several shelf areas from the surface to 500 m that are weaker or absent in other climatologies of comparable resolution. These features are a signature of the region's boundary currents and are consistent with high-resolution research ship surveys. Their clear representation in ATLAS demonstrates the important role that marine mammal-borne sensors can have in more accurately constraining the climatological temperature structure in regions undersampled by Argo. This is particularly relevant given recent work that shows restoring an ocean-only hindcast back to a climatology with a poorly defined boundary current can enhance rather than restrain model drift [Rattan *et al.*, 2010]. In the future, as more marine mammal-borne sensors are deployed north of Iceland, we plan to extend our analysis to this region including a description of the EGC near the relatively data sparse Belgica Bank region to the north-east of Greenland.

[16] To conclude, the new ATLAS dataset has revealed features in the high latitude North-West Atlantic lacking in other climatologies and demonstrates the value of marine mammal-borne sensor data at a time of rapid change.

[17] **Acknowledgments.** We thank Penny Holliday for beneficial discussions of this research, which is funded by UK Natural Environment Research Council grant NE/H01103X/1. The marine mammal deployments were funded by Fisheries and Oceans Canada Centre of Expertise in Marine Mammalogy (CEMAM), DFO's International Governance and Atlantic Seal Research Programs, Canada's International Polar Year Program and the Greenland Institute of Natural Resource. Enquiries about the marine mammal data should be made to GS (garry.stenson@dfo-mpo.gc.ca). Simon Good provided data on the number of observations in EN3.

[18] The Editor thanks an anonymous reviewer for their assistance in evaluating this paper.

References

- Andersen, J. M., Y. F. Wiersma, G. Stenson, M. O. Hammill, and A. Rosing-Asvid (2010), Movement patterns of hooded seals (*Cystophora cristata*) in the northwest Atlantic Ocean during the post-moult and pre-breed seasons, *J. Northwest Atl. Fish. Sci.*, *42*, 1–11, doi:10.2960/J.v42.m649.
- Bacon, S., G. Reverdin, I. G. Rigor, and H. M. Snaith (2002), A freshwater jet on the east Greenland shelf, *J. Geophys. Res.*, *107*(C7), 3068, doi:10.1029/2001JC000935.
- Boehme, L., and U. Send (2005), Objective analyses of hydrographic data for referencing profiling float salinities in highly variable environments, *Deep Sea Res., Part II*, *52*, 651–664, doi:10.1016/j.dsr2.2004.12.014.
- Boehme, L., M. P. Meredith, S. E. Thorpe, M. Biuw, and M. Fedak (2008a), Antarctic Circumpolar Current frontal system in the South Atlantic: Monitoring using merged Argo and animal-borne sensor data, *J. Geophys. Res.*, *113*, C09012, doi:10.1029/2007JC004647.
- Boehme, L., S. E. Thorpe, M. Biuw, M. Fedak, and M. P. Meredith (2008b), Monitoring Drake Passage with elephant seals: Frontal structures and snapshots of transport, *Limnol. Oceanogr.*, *53*, 2350–2360, doi:10.4319/lo.2008.53.5_part_2.2350.
- Boehme, L., P. L. Lovell, M. Biuw, F. Roquet, J. Nicholson, S. E. Thorpe, M. Meredith, and M. A. Fedak (2009), Animal-borne CTD-Satellite Relay Data Loggers for real-time oceanographic data collection, *Ocean Sci.*, *5*, 685–695, doi:10.5194/os-5-685-2009.
- Chanut, J., et al. (2008), Mesoscale eddies in the Labrador Sea and their contribution to convection and restratification, *J. Phys. Oceanogr.*, *38*, 1617–1643, doi:10.1175/2008JPO3485.1.
- Charrassin, J.-B., et al. (2008), Southern Ocean frontal structure and sea-ice formation rates revealed by elephant seals, *Proc. Natl. Acad. Sci. U. S. A.*, *105*, 11,634–11,639, doi:10.1073/pnas.0800790105.
- Cuny, J., P. B. Rhines, and R. Kwok (2005), Davis Strait volume, freshwater and heat fluxes, *Deep Sea Res., Part I*, *52*, 519–542, doi:10.1016/j.dsr.2004.10.006.
- Fratantoni, P. S., and R. S. Pickart (2007), The western North Atlantic Shelfbreak Current system in summer, *J. Phys. Oceanogr.*, *37*, 2509–2533, doi:10.1175/JPO3123.1.
- Holliday, N. P., A. Meyer, S. Bacon, S. Alderson, and B. A. de Cuevas (2007), The retroflexion of part of the East Greenland Current at Cape Farewell, *Geophys. Res. Lett.*, *34*, L07609, doi:10.1029/2006GL029085.
- Ingleby, B., and M. Huddleston (2007), Quality control of ocean temperature and salinity profiles—historical and real-time data, *J. Mar. Syst.*, *65*, 158–175, doi:10.1016/j.jmarsys.2005.11.019.
- Kulan, N., and P. G. Myers (2009), Comparing two climatologies of the Labrador Sea: Geopotential and isopycnal, *Atmos. Ocean*, *47*, 19–39, doi:10.3137/OC281.2009.
- Laidre, K. L., M. P. Heide-Jørgensen, W. Ermold, and M. Steele (2010), Narwhals document continued warming of southern Baffin Bay, *J. Geophys. Res.*, *115*, C10049, doi:10.1029/2009JC005820.
- Levitus, S., et al. (1998), *World Ocean Database 1998*, NOAA Atlas NESDIS 18, U.S. Gov. Print. Off, Washington, D. C.
- Levitus, S., J. I. Antonov, T. P. Boyer, R. A. Locarnini, H. E. Garcia, and A. V. Mishonov (2009), Global ocean heat content 1955–2008 in light of recently revealed instrumentation problems, *Geophys. Res. Lett.*, *36*, L07608, doi:10.1029/2008GL037155.
- Rattan, S., P. G. Myers, A.-M. Treguier, S. Theeten, A. Biastoch, and C. Böning (2010), Towards an understanding of Labrador Sea salinity drift in eddy-permitting simulations, *Ocean Modell.*, *35*, 77–88, doi:10.1016/j.ocemod.2010.06.007.
- Rudels, B., E. Fahrbarch, J. Meincke, G. Budéus, and P. Eriksson (2002), The East Greenland Current and its contribution to the Denmark Strait overflow, *ICES J. Mar. Sci.*, *59*, 1133–1154, doi:10.1006/jmsc.2002.1284.
- Straneo, F., G. S. Hamilton, D. A. Sutherland, L. A. Stearns, F. Davidson, M. O. Hammill, G. B. Stenson, and A. Rosing-Asvid (2010), Rapid circulation of warm subtropical waters in a major glacial fjord in East Greenland, *Nat. Geosci.*, *3*, 182–186, doi:10.1038/ngeo764.
- Stroeve, J., M. Holland, W. Meier, T. Scambos, and M. Serreze (2007), Arctic sea ice decline: Faster than forecast, *Geophys. Res. Lett.*, *34*, L09501, doi:10.1029/2007GL029703.
- Sutherland, D. A., and R. S. Pickart (2008), The East Greenland Coastal Current: Structure, variability, and forcing, *Prog. Oceanogr.*, *78*, 58–77, doi:10.1016/j.pocean.2007.09.006.
- Tang, C. C. L., C. K. Ross, T. Yao, B. Petrie, B. M. DeTracey, and E. Dunlap (2004), The circulation, water masses and sea-ice of Baffin Bay, *Prog. Oceanogr.*, *63*, 183–228, doi:10.1016/j.pocean.2004.09.005.

L. Boehme, Sea Mammal Research Unit, University of St. Andrews, Saint Andrews KY16 8LB, UK. (lb284@st-andrews.ac.uk)

F. J. M. Davidson and G. B. Stenson, Fisheries and Oceans Canada, PO Box 5667, St. John's, NL A1C 5X1, Canada. (fraser.davidson@dfo-mpo.gc.ca; garry.stenson@dfo-mpo.gc.ca)

J. P. Grist and S. A. Josey, National Oceanography Centre, European Way, Southampton SO14 3ZH, UK. (jeremy.grist@noc.ac.uk; simon.a.josey@noc.ac.uk)

M. O. Hammill, Maurice Lamontagne Institute, Fisheries and Oceans Canada, PO Box 1000, Mont-Joli, QC G5H 3Z4, Canada. (mike.hammill@dfo-mpo.gc.ca)

M. P. Meredith, British Antarctic Survey, High Cross, Madingley Road, Cambridge CB3 0ET, UK. (mmm@bas.ac.uk)